Article

Cell Reports

Vascular Mural Cells Promote Noradrenergic Differentiation of Embryonic Sympathetic Neurons

Graphical Abstract

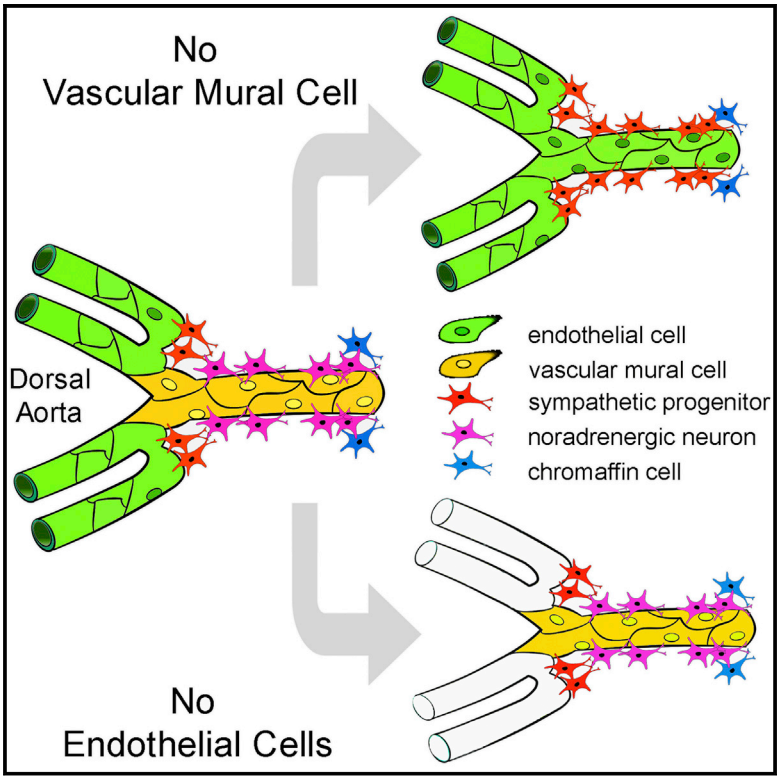

Highlights

- SN precursors close to the DA acquire NA markers (TH and DβH)
- NA differentiation requires vascular remodeling and VMC recruitment
- Inhibition of PDGFR signaling prevents VMC recruitment and NA differentiation
- VMC are sufficient to direct SN development in absence of endothelial cells

Authors

Vitor Fortuna, Luc Pardanaud, Isabelle Brunet, ..., Massimo M. Santoro, Stefania Nicoli, Anne Eichmann

Correspondence

stefania.nicoli@yale.edu (S.N.), anne.eichmann@yale.edu (A.E.)

In Brief

Fortuna et al. show that neurovascular interactions between the aorta and sympathetic precursors are mediated by PDGFR-driven mural cell recruitment that promotes noradrenergic differentiation.

Fortuna et al., 2015, Cell Reports *11*, 1786–1796
June 23, 2015
http://dx.doi.org/10.1016/j.celrep.2015.05.028

CellPress

OPEN ACCESS
CellPress

Cell Reports
Article

Vascular Mural Cells Promote Noradrenergic Differentiation of Embryonic Sympathetic Neurons

Vitor Fortuna,[1,2] Luc Pardanaud,[3] Isabelle Brunet,[3] Roxana Ola,[1] Emma Ristori,[1] Massimo M. Santoro,[4,5] Stefania Nicoli,[1,*] and Anne Eichmann[1,3,6,*]

[1]Department of Internal Medicine, Yale Cardiovascular Research Center, Yale University School of Medicine, New Haven, CT 06510, USA
[2]Health Science Institute, Federal University of Bahia, Salvador 40110-902, Brazil
[3]CNRS UMR7241, INSERM U1050, Center for Interdisciplinary Research in Biology (CIRB), Collège de France, Paris 75005, France
[4]Department of Molecular Biotechnology and Health Sciences, Molecular Biotechnology Center, University of Torino, 10126 Torino, Italy
[5]VIB Vesalius Research Center, KU Leuven, 3000 Leuven, Belgium
[6]Department of Cellular and Molecular Physiology, Yale University School of Medicine, New Haven, CT 06510, USA
*Correspondence: stefania.nicoli@yale.edu (S.N.), anne.eichmann@yale.edu (A.E.)
http://dx.doi.org/10.1016/j.celrep.2015.05.028

SUMMARY

The sympathetic nervous system controls smooth muscle tone and heart rate in the cardiovascular system. Postganglionic sympathetic neurons (SNs) develop in close proximity to the dorsal aorta (DA) and innervate visceral smooth muscle targets. Here, we use the zebrafish embryo to ask whether the DA is required for SN development. We show that noradrenergic (NA) differentiation of SN precursors temporally coincides with vascular mural cell (VMC) recruitment to the DA and vascular maturation. Blocking vascular maturation inhibits VMC recruitment and blocks NA differentiation of SN precursors. Inhibition of platelet-derived growth factor receptor (PDGFR) signaling prevents VMC differentiation and also blocks NA differentiation of SN precursors. NA differentiation is normal in *cloche* mutants that are devoid of endothelial cells but have VMCs. Thus, PDGFR-mediated mural cell recruitment mediates neurovascular interactions between the aorta and sympathetic precursors and promotes their noradrenergic differentiation.

INTRODUCTION

The sympathetic nervous system (SNS) controls involuntary body functions such as circulation, respiration, body temperature, sweating, digestion, and metabolism (Kuntz, 1948). SNS activation elevates blood pressure by increasing heart rate and peripheral vascular resistance. Cardiovascular responses to sympathetic activation are mediated by postganglionic sympathetic neurons (hereafter abbreviated SNs) that innervate visceral, vascular, and cardiac smooth muscle throughout the body. Dysfunction of the SNS leads to pathologies including congestive heart failure and hypertension, which affect millions of people worldwide. Understanding how SNs develop may offer new approaches to combat these diseases.

SNs are derived from the trunk neural crest (NC), a highly migratory multipotent cell population in developing vertebrate embryos (Le Douarin et al., 1981). NC cells delaminate from the dorsal neural tube (NT) and migrate along specific pathways to generate SNs and various additional cell types, including sensory neurons of dorsal root ganglia, ganglion satellite cells, Schwann cells of peripheral nerves, and melanocytes (Le Douarin and Kalcheim, 1999). NC cells forming the sympathetic ganglia migrate ventrally toward the main embryonic artery, the dorsal aorta (DA), where they differentiate and acquire a noradrenergic (NA) phenotype (Bronner-Fraser, 1986; Nitzan et al., 2013; Stern et al., 1991).

Here, we ask if the DA instructs early SN development in zebrafish embryos. SN development is conserved between vertebrate species and involves a series of differentiation steps and gene regulators that transform NC progenitors into mature SNs (An et al., 2002; Apostolova and Dechant, 2009; Guo et al., 1999; Rohrer, 2011; Stewart et al., 2010). Sequential expression of a number of transcription factors, starting with Mash1 (Zash-1 in zebrafish) (Allende and Weinberg, 1994) and Phox2b, followed by Insm1, Hand2, Phox2a, and Gata2, direct SN progenitor survival and proliferation, NA differentiation, and maintenance of differentiated properties (Howard et al., 2000; Rohrer, 2011; Tsarovina et al., 2004; Wildner et al., 2008). Tracking of zebrafish and avian NC cells showed that restriction to a neural fate already occurs before migration from the NT (McKinney et al., 2013, Raible and Eisen, 1996; Shtukmaster et al., 2013). However, misrouting of sympathetic NC progenitors does not result in ectopic NA neurons, indicating that migrating NC cells are not yet determined toward the SN lineage (Krispin et al., 2010, Stern et al., 1991). NA differentiation of sympathetic progenitors starts once they have reached the vicinity of the DA. Here, they acquire postmitotic and NA markers, including the expression of dopamine-beta hydroxylase (DβH) and tyrosine hydroxylase (TH), the enzyme catalyzing the rate-limiting step in catecholamine biosynthesis, followed by catecholamine storage (Flatmark, 2000; Saito et al., 2012).

SN progenitor migration and differentiation are controlled by three cytokine families, bone morphogenetic proteins (BMPs), the chemokine stromal-cell-derived factor-1 (SDF1, also called

CXCL12), and Neuregulin 1 (NRG1) of the epidermal growth factor (EGF) family (Kasemeier-Kulesa et al., 2010; McPherson et al., 2000; Reissmann et al., 1996; Schneider et al., 1999; Shah et al., 1996; Woldeyesus et al., 1999). BMP-2, BMP-4, and BMP-7 are expressed in and around the DA and are required for SN differentiation as shown by BMP treatment of cultured NC stem cells, which instructs Mash1 expression and sympathetic differentiation (Shah et al., 1996), and by application of the BMP antagonist noggin, which prevented SN differentiation in chick embryos (Schneider et al., 1999). BMPs do not directly affect SN progenitor migration, as shown by lack of effects of BMP receptor inhibition in NC cells; instead, BMPs are required for the expression of the chemoattractants SDF1 and NRG1 in the para-aortic mesenchyme (Saito et al., 2012). Furthermore, BMPs are cell-autonomously required for SN survival, as shown by deletion of the BMP receptor Alk3 in NC cells in mice, which leads to block of Phox2b expression and SN death (Morikawa et al., 2009).

The data summarized above provide "guilt by association" circumstantial evidence that the DA is involved in SN differentiation. It is, however, unclear if the presence of the DA is required and sufficient to induce SN differentiation, and if so, which step of SN differentiation requires DA-derived signals. SN differentiation may require signals from the flowing blood, from endothelial cells or from vascular mural cells (VMCs) surrounding the DA. In fact, vascular maturation and VMC recruitment around the DA roughly coincide temporally with sympathetic ganglion formation, and BMP-induced Mash1 expression in cultured NC cells occurs concomitantly with VMC formation (Shah et al., 1996). BMPs also promote TH expression in co-cultures of DA with NC cells (Reissmann et al., 1996; Schneider et al., 1999).

However, whether VMCs are required for SN differentiation has never been experimentally addressed. We here investigate SN development in zebrafish embryos, a uniquely suited model that allows embryo survival in the absence of endothelial cells and blood flow. We show that SNs develop adjacent to the DA from *zash-1a*$^{+}$ SN precursors and that their NA differentiation requires vascular maturation and recruitment of VMCs via platelet-derived growth factor receptor (PDGFR) signaling. Blockade of PDGFR signaling inhibits VMC differentiation and blocks NA differentiation of SN precursors. Furthermore, VMCs present in *cloche* mutants devoid of endothelial cells and blood flow are sufficient to direct normal NA differentiation. Thus, VMC recruitment to the DA via PDGFR signaling directs the acquisition of NA properties of SNs.

RESULTS

SNs Develop in Close Proximity to the DA

To monitor the development of SNs and their relationship to blood vessels, we performed whole-mount immunostaining with antibodies specific for the neuronal marker HuC/D (hereafter HU) and TH in *Tg(kdrl:EGFP)*^{la116} transgenic embryos carrying an endothelial-specific EGFP reporter (An et al., 2002; Choi et al., 2007; Park et al., 2000). Double-positive HU and TH^{+} SNs were first observed at 48 hr post-fertilization (hpf) immediately adjacent to the DA, just posterior to its Y-shaped bifurcation into right and left lateral dorsal aorta (LDA) and juxtaposed on each side of the kidney glomerular region (Figures 1A, S1A, and S1B). We counted two double-positive HU^{+}/TH^{+} SNs on each side of the DA at 48 hpf (Figures 1A and 1D, white arrows). A few hours later at 60 hpf, the SN number had increased significantly to ~14 SNs arranged in two parallel rows along the DA and its bifurcation to the LDA (Figures 1B and 1D, white arrows). The increase in SNs between 48 and 60 hpf coincided temporally with the connection of the LDA to the fifth and sixth aortic arches (AA), which completes remodeling of the embryonic arterial network (Siekmann et al., 2009, Nicoli et al., 2010) (Figure 1B, yellow arrow). At 72 hpf, three distinct groups of SNs were found along the LDA-DA axis. The rostralmost cluster was located next to the LDA-DA connection; this cluster contained the highest numbers of SNs (Figures 1C–1E). The central cluster was located around the kidney glomerular region and interspersed with chromaffin cells (HU^{-}/TH^{+}), and the posterior cluster developed at the level of the first intersegmental vessel (ISV) in the proximal trunk region (Figures 1C–1E and S1B). SNs were not detected anywhere else in the embryo at these stages, in agreement with previous reports (An et al., 2002; Guo et al., 1999; Holzschuh et al., 2003).

To confirm these results, we time-lapse imaged *Tg(dβh:EGFP);(kdrl:ras-mcherry)*^{s916}, expressing mCherry under the *kdrl*-endothelial promoter and EGFP under control of the *dβh* promoter (Zhu et al., 2012). Like TH^{+} neurons, EGFP expression first became detectable around the glomerular region next to the DA at 48 hpf and at the LDA-DA connection at ~60 hpf (Figures S1C–S1E), indicating that differentiation of DβH^{+} cells takes place in situ at these sites. Taken together, these data show that the appearance of the first SNs in the zebrafish embryo coincides with vascular remodeling of the DA bifurcation (Anderson et al., 2008; Guo et al., 1999; Holzschuh et al., 2003; Nicoli et al., 2010; Stewart et al., 2010).

We noted that HU^{+} neurons were already present at the LDA-DA connection at 48 hpf, 12 hr prior to the emergence of TH^{+} cells in this region (Figures 1A and 1B), suggesting that these HU^{+} cells might subsequently differentiate into TH^{+} SNs. In agreement with this idea, in situ hybridization with antisense riboprobes specific for the sympathetic precursor markers *zash-1a* and *phox-2b* (Lucas et al., 2006; Stewart et al., 2006) showed that the first *zash-1a* and *phox-2b* RNA-expressing cells appeared at 40 hpf in the glomerular region, and as their number increased rostrally and caudally at 48 and 60 hpf (Figures 2A–2C and S2), the centrally located progenitors in the glomerular region acquired *th* RNA expression at 48 hpf (Figure S2). These results are consistent with a stepwise model of SN development in which sympathetic precursors aggregate next to the DA, acquire neuronal markers, and subsequently undergo NA differentiation (Figure 2D).

NA Differentiation of SN Precursors Requires Flow-Induced Vascular Maturation

Since the emergence of HU^{+}/TH^{+} SNs occurred at the same time as LDA remodeling and maturation of the arterial network, we reasoned that blood-flow-induced vascular maturation could affect neuronal and/or NA differentiation of sympathetic precursors. To test this hypothesis, we first interrupted blood flow by targeting the *tnnt2* gene, which encodes cardiac troponin T

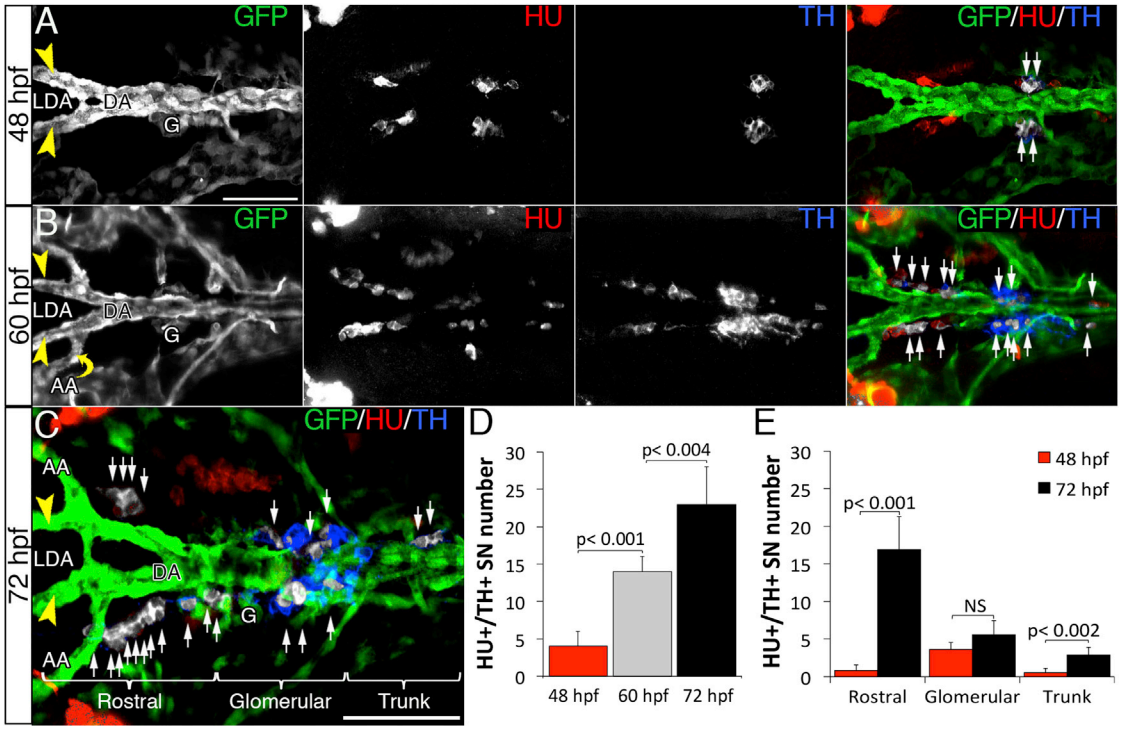

Figure 1. SNs Develop Next to the DA in Zebrafish Embryos

(A–C) Dorsal views (anterior is to the left) of whole-mount *Tg(kdrl:EGFP)*^{la116} zebrafish embryos between the LDA (arrowheads) and DA connection and the glomerular region (G) at the indicated time points. Immunostaining with antibodies to detect GFP (vessels, green), Hu C/D (post-mitotic neurons, red), and tyrosine hydroxylase enzyme (TH) (catecholaminergic marker, blue). (A and B) HU$^+$/TH$^+$ SNs are pseudocolored in white (arrows) in the merged confocal images. (C) Brackets mark the three clusters (rostral, glomerular, and trunk) of SNs organized around DA.

(D) Quantification of total number of double HU$^+$/TH$^+$ cells at 48, 60, and 72 hpf.

(E) Quantification of double HU$^+$/TH$^+$ cells organized in three clusters around the DA at 48 and 72 hpf. Data were calculated from three independent experiments. NS, not significant; error bars indicate SD.

DA, dorsal aorta; LDA, lateral dorsal aorta; AA, aortic arch; G, glomerulus; hpf, hours post-fertilization. Scale bars, 75 μm (A–C). See also Figure S1.

(Sehnert et al., 2002). *Tnnt2* morpholino knockdown leads to failure to initiate heartbeat, and embryos consequently lack circulatory blood flow (Bussmann et al., 2011; Sehnert et al., 2002). At 48 hpf, zebrafish *tnnt2* morphants have intact trunk vasculature, as shown previously (Isogai et al., 2003), but their LDA-DA morphology was severely disorganized (Figure 3 and data not shown). In these morphants, TH$^+$ SNs were present at 48 hpf, although they seemed ectopically localized when compared to control embryos with blood flow (Figures 3A–3C, white arrows). At 60 hpf, the number of TH$^+$ SNs was significantly reduced when compared to controls (Figures 3D–3F, white arrows), consistent with the idea that circulatory blood flow might affect SN differentiation and patterning. However, the major vessel morphology defects observed in the LDA region of *tnnt2* morphants rendered interpretation of these experiments difficult.

We next reversibly arrested circulatory blood flow during defined time periods and assessed effects on SN development using nifedipine, an inhibitor of myofibrillar Ca^{2+}-ATPases (Bussmann et al., 2011). Treatment with 40 μM nifedipine at 40 hpf followed by analysis of SNs 8 hr later showed no significant difference in TH$^+$/HU$^+$ SN number between control and treated groups, although heartbeat was arrested (not shown) and LDA-DA vessel morphology was altered (Figures 4A, 4B, and 4H, white arrows). Treatment of embryos with nifedipine at 48 hpf showed that 12 hr later, HU$^+$ neurons were present next to the LDA-DA connection, but the number of HU$^+$/TH$^+$ SNs was significantly reduced (Figures 4C, 4D, and 4H, white arrows). When the embryos were submitted to 40 μM nifedipine starting at 60 hpf and examined for the presence of SNs 12 hr later, the number of HU$^+$/TH$^+$ SNs between controls and treated groups was similar (Figures 4E, 4F, and 4H). Similar results were obtained with no-flow embryos generated by treatment with a myosin-ATPase inhibitor (2, 3-butanedione-2-monoxime [BTM], 20 mM; Figures S3A–S3H). To test reversibility of flow arrest, we repeated the nifedipine treatment for 12 hr starting at 48 hpf and then removed the drug at 60 hpf until 72 hpf. Nifedipine withdrawal completely restored NA differentiation (Figures 4G and 4H). In contrast to TH expression, nifedipine did not affect expression of *zash-1a* (Figures S3I and S3J), demonstrating that blood-flow arrest specifically affects NA differentiation of SNs between 48 and 60 hpf.

Vascular Mural Cell Coverage Is Critical for NA Differentiation

While NA differentiation of SNs occurred next to the LDA-DA connection, SNs were always located at a small distance from

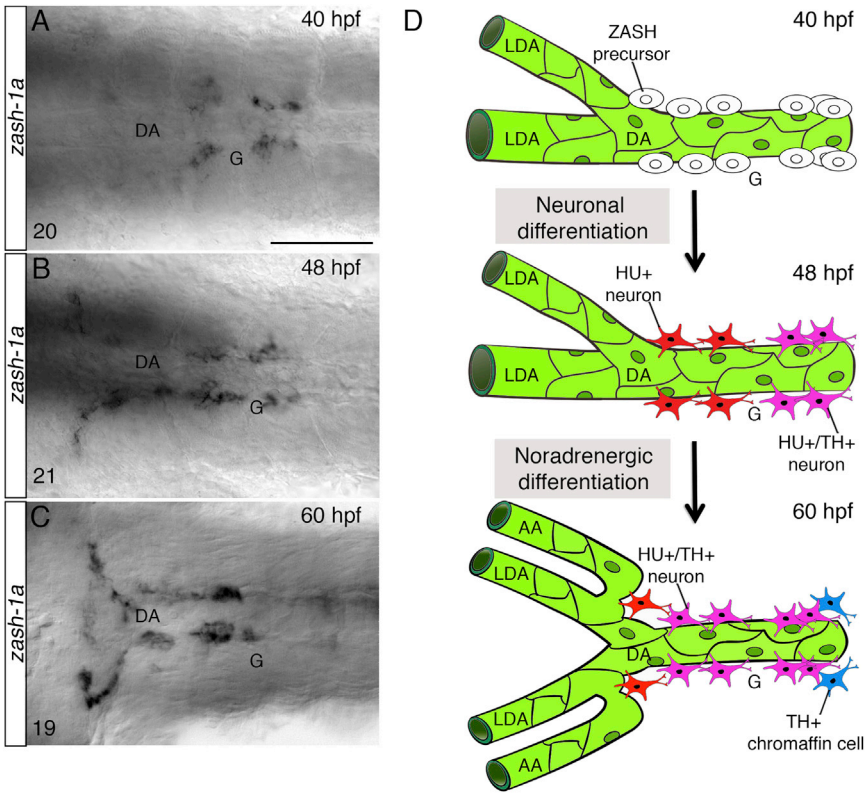

Figure 2. Early SN Precursors Develop Next to the DA

(A–C) Whole-mount in situ hybridizations with antisense riboprobe specific for *zash-1a* RNA expression at the indicated time points. Images are ventral views (anterior is to the left) of the region between the LDA-DA connection (left) and the glomerular region (G) after dissection of the yolk sac. *Zash-1a*$^+$ sympathetic precursors are present around the DA at 40 hpf (A). At 48 hpf (B) and 60 hpf (C), *zash-1a* expression expands to more anterior and posterior regions. The number of embryos observed is indicated at the bottom left.

(D) Schematic representation of SN development. At 40 hpf, zash-1a+ sympathetic precursors differentiate next to the DA. At 48 hpf, they acquire HU expression and some of them become TH$^+$. At 60 hpf, most of them have acquired TH expression.

DA, dorsal aorta; LDA, lateral dorsal aorta; AA, aortic arch; G, glomerulus; hpf, hours post-fertilization. Scale bar, 75 μm (A–C). See also Figure S2.

the endothelial cells lining the DA, suggesting that another cell type might be interposed between endothelial cells and SNs. During embryonic development, larger vessels recruit VMCs that play an essential part in the stabilization and maturation of new vascular networks. Since the earliest VMCs in zebrafish embryos emerge at the LDA-DA connection (Santoro et al., 2009; Seiler et al., 2010), we hypothesized that VMC recruitment might trigger the acquisition of NA identity.

Labeling of *Tg(kdrl:EGFP)*^{la116} embryos with specific antibodies that recognize zebrafish Transgelin encoding Sm22alpha-b (Santoro et al., 2009) and TH showed that the earliest Transgelin expression was seen at 48 hpf in the area where TH$^+$ SNs differentiate between the LDA-DA connection and the glomerular region (Figure 5A). Transgelin$^+$ VMCs were only found in this region, and Transgelin expression increased between 48 hpf and 60 hpf (Figure 5B). Notably, high-magnification images of double-positive HU$^+$/TH$^+$ cells showed Transgelin$^+$ VMCs in proximity to SNs (Figures 5C and 5D, white arrows). These data show that VMC coverage coincides spatially and temporally with NA differentiation of SNs. Nifedipine-induced flow arrest between 48 and 60 hpf reduced VMC coverage along with NA differentiation (Figures 5E and 5F), suggesting that VMC coverage around the LDA-DA connection might be flow dependent and affect NA differentiation.

PDGFR Tyrosine Kinase Inhibition Reduces VMC Coverage and NA Differentiation

To examine if VMCs were functionally required for NA differentiation, we decided to block PDGFRβ, which is expressed in VMCs, but not in SNs, in zebrafish and mouse embryos (Figure S4) and plays a role in VMC recruitment (Armulik et al., 2005; Eberhart et al., 2008; Kim et al., 2010). We injected embryos at one cell post-fertilization with a heat-shock-inducible dominant-negative *pdgfrβ* construct where the intracellular *pdgfrβ* kinase domain was substituted with yellow fluorescent protein (YFP) (Wiens et al., 2010). Heat shock was performed at 24 hpf and embryos were selected for dnpdgfrβ-YFP expression at 60 hpf. In these embryos, the LDA-DA connection occurred normally (Figures S5A and S5B). Transgelin staining around the DA was reduced (Figures 6A, 6B, and 6H, yellow arrowhead), and staining with HU and TH antibodies revealed a significant reduction in the number of TH$^+$ SNs (Figures 6A, 6B, and 6G, white arrows). Next, zebrafish *Tg(kdrl:EGFP)*^{la116} embryos at 48 hpf were treated with increasing concentrations of PDGFR tyrosine kinase inhibitor V (InhV) (Eberhart et al., 2008; Kim et al., 2010) or DMSO as control. After 12 hr, treatment with InhV resulted in a dose-dependent reduction in the number of TH$^+$ SNs (Figures S5C–S5E), which was statistically significant in embryos treated with 1.0 μM InhV and similar to effects of the dominant-negative pdgfrβ construct (Figures 6C, 6D, 6G, and 6H). We also observed a reduction of Transgelin$^+$ VMC coverage in embryos treated with 1.0 μM InhV at 60 hpf (Figures 6C, 6D, and 6H, yellow arrowhead). To test reversibility of pharmacological PDGFR inhibition, we repeated the InhV treatment between 48 and 60 hpf and then removed the drug between 60 and 72 hpf. InhV withdrawal completely restored Transgelin expression and rescued NA differentiation (Figures 6E–6H). We did not observe any impaired blood-flow circulation or defects in LDA-DA remodeling in InhV-treated embryos (Wiens et al., 2010). Importantly, neither the expression of *zash-1a* nor the number of HU$^+$ neurons was affected by InhV or the dominant-negative pdgfrβ construct

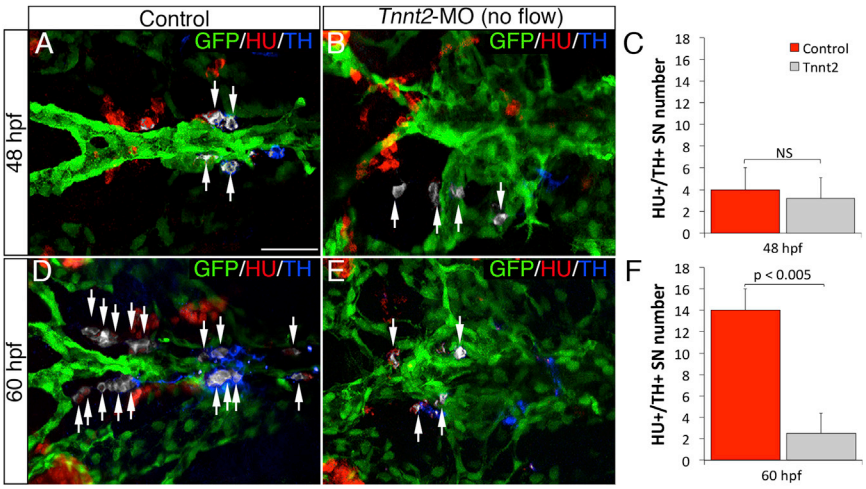

Figure 3. Absence of Blood Flow Perturbs Vascular Maturation and SN Differentiation

(A, B, D, and E) Confocal images of control (A and D) or *tnnt2* morpholino-injected (B and E) *Tg(kdrl:EGFP)*^{la116} zebrafish embryos immunostained for GFP (green), HU (red), and TH (blue). Dorsal views (anterior is to the left). HU$^+$/TH$^+$ SNs are pseudocolored in white and indicated (arrows). *Tnnt2* morphants display defective remodeling of the LDA-DA and misalignment of HU$^+$/TH$^+$ neurons.

(C and F) Quantification of SNs (HU$^+$/TH$^+$) in control and *tnnt2* morpholino-injected embryos at 48 (C) and 60 hpf (F). Data were calculated from three independent experiments.

NS, not significant; error bars indicate SD. Hpf, hours post-fertilization. Scale bar, 50 μm (A, B, D, and E).

(Figures S5H and S5I). In addition to HU$^+$/TH$^+$ SNs, the number of HU$^-$/TH$^+$ cells in the glomerular region was also reduced by flow arrest or PDGFR inhibition (Figure S5I). These data show that decreasing coverage by Transgelin$^+$ VMCs by blocking PDGFR signaling selectively inhibits NA differentiation of SNs, but not earlier SN migration or specification.

VMCs Are Sufficient for NA Differentiation

We next asked if besides VMCs, other signals derived from endothelium or from blood flow might be required for SN differentiation. To address this point, we took advantage of the zebrafish *cloche* mutant (*clo*^{s5}), which lacks all endothelial precursors in the head and trunk regions (Santoro et al., 2009; Stainier et al., 1995). Interestingly, whole-mount immunostaining analysis of HU and TH markers in *clo*^{s5} mutant embryos revealed no significant differences in *phox-2b* expression or the number and position of HU$^+$ and HU$^+$/TH$^+$ SNs between mutants and control siblings at 48 and 60 hpf (Figures 7A, 7B, 7G, and S6A–S6F). Thus, the NA differentiation of SNs in *clo*^{s5} mutants proceeds normally despite the absence of endothelial cells. Notably, *clo*^{s5} mutants showed Transgelin$^+$ cells in the region corresponding to the DA floor and in the anterior cervical region between somites 1 and 4, indicating that *clo*^{s5} mutants exhibit fairly normal VMC development (Figures 7B, 7H, and S6C–S6F). InhV treatment between 48 and 60 hpf reduced Transgelin expression and concomitantly decreased the number of TH$^+$/HU$^+$ SNs, and InhV washout between 48 and 60 hpf restored both Transgelin expression and the number of HU$^+$/TH$^+$ SNs (Figures 7C–7H). These data show that Transgelin$^+$ VMCs are sufficient to mediate NA differentiation in the absence of endothelial cells and blood flow.

If VMCs were critical for NA differentiation, then we expected that VMC coverage should be correlated temporally with the appearance of TH$^+$ SNs in other species, including mouse and avian embryos. In embryonic day 3.5 (E3.5) quail embryos and E10.5 mouse embryos, staining with anti-SMA and anti-TH showed that TH$^+$ SNs aggregated next to VMC-covered regions of the DA (Figures S7A and S7B). Since both SN differentiation and DA morphogenesis occur in a cranio-caudal direction, analysis of more posterior levels of the same E10.5 mouse embryo shows earlier stages of DA morphogenesis and SN differentiation. In regions next to the hindlimb, where the bilateral DA fused into a single tube, TH$^+$ cells were already present next to the DA, but they aggregated next to regions that were not covered with SMA$^+$ cells (Figure S7C), indicating that if VMCs are required for differentiation of TH$^+$ SNs, they might be more immature cells. Indeed, double staining with NG2, a marker for immature VMCs and pericytes, and TH showed that TH$^+$ cells formed next to NG2$^+$ areas of the DA (Figure S7D). These data suggest that VMC recruitment and differentiation of TH$^+$ SNs temporally coincide in zebrafish, avian, and mammalian embryos.

DISCUSSION

We use the zebrafish system to test the requirement of the DA in SN development and dissect the cellular and molecular mechanisms regulating neurovascular interactions between the DA and SN precursors. Previous work and the present study show that early events of SN development are highly conserved among zebrafish, avian, and mouse, including NC migration of SN precursors toward the DA and molecular signals inducing SN differentiation, such as BMPs and the transcription factors Zash-1, Phox2a, Phox2b, GATA3, and dHand (Apostolova and Dechant, 2009; Young et al., 2011). We here confirm that the first TH$^+$/HU$^+$ SNs develop adjacent to the DA at 48 hpf (An et al., 2002; Guo et al., 1999). Acquisition of TH immunoreactivity was mirrored by acquisition of DβH fluorescence in transgenic embryos expressing dβh:EGFP, indicating that TH immunolabeling faithfully detects SNs (Zhu et al., 2012). These SNs are thought to belong to the superior cervical ganglion (SCG) and lie just anterior to the kidney glomerulus, where they are interspersed with HU$^-$/TH$^+$ chromaffin cells of the adrenal medulla (Stewart et al., 2010).

The major finding of this study is that VMCs promote NA differentiation of SN precursors (Figure 7G). We show that Zash1a$^+$/HU$^+$ SN precursors are present next to the DA 12 hr prior to acquisition of DβH and TH, indicating a critical time window required for NA differentiation of these precursors. This period

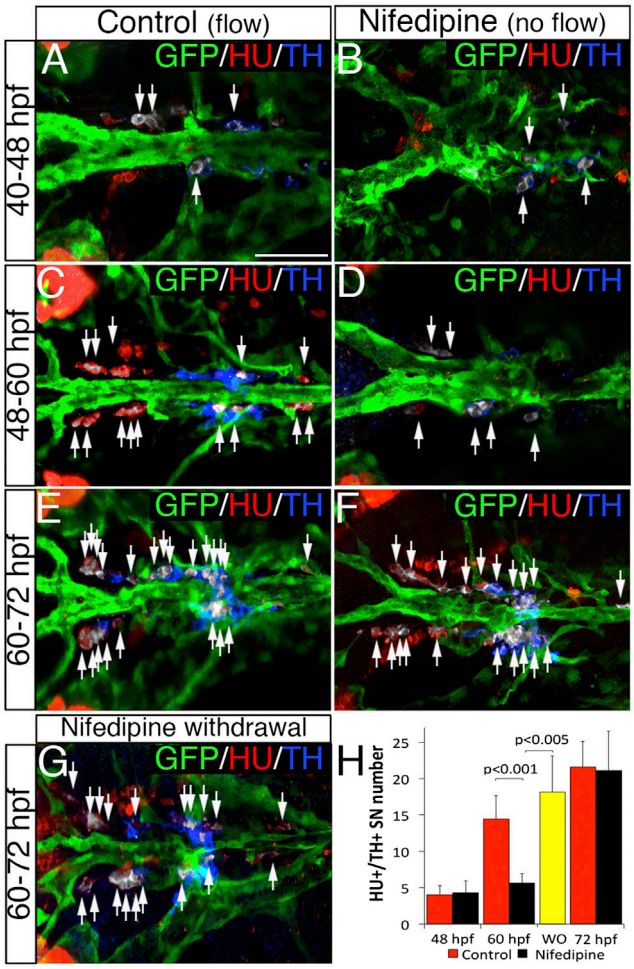

Figure 4. NA Differentiation of SNs Requires Blood Flow

(A–F) Dorsal views (anterior is to the left) of control (A, C, and E) or nifedipine-treated (B, D, and F) *Tg(kdrl:EGFP)*^{la116} zebrafish embryos. HU$^+$/TH$^+$ SNs are pseudocolored in white and indicated (arrows). Nifedipine was used to arrest blood flow during the periods indicated on the left. Treatment with 40 μM Nifedipine from 40–48 hpf or from 60–72 hpf does not affect the NA differentiation of SNs (A, B, E, F, and H). Nifedipine treatment from 48 to 60 hpf significantly decreases NA differentiation of SNs (C, D, and H).

(G) After nifedipine exposure between 48 and 60 hpf, the drug was withdrawn and embryos were maintained in control conditions for an additional 12 hr (60–72 hpf). NA differentiation recovered following nifedipine withdrawal.

(H) Quantification of HU$^+$/ TH$^+$ SNs in control (red bars), nifedipine-treated (black bars), and nifedipine-withdrawal (WO) (yellow bar) embryos. Data were calculated from three independent experiments.

Error bars indicate SD. Hpf, hours post-fertilization. Scale bar, 50 μm (A–G). See also Figure S3.

(48–60 hpf) temporally coincides with flow-dependent LDA-DA remodeling and recruitment of Transgelin$^+$ VMCs (Anderson et al., 2008; Nicoli et al., 2010). One of the advantages of the zebrafish embryo is that embryos can survive in the absence of blood flow for several days (Isogai et al., 2003, Serluca et al., 2002), allowing us to directly test if blood-flow arrest can inhibit neuronal and/or NA differentiation of sympathetic precursors. We found that reversible flow arrest induced by pharmacological inhibition of myofibrillar Ca^{2+}-ATPases or a myosin-ATPase inhibitor (Anderson et al., 2008; Li et al., 2008) inhibited NA, but not neuronal differentiation of SN precursors. Flow arrest affected NA differentiation only during the critical 12-hr period between 48 and 60 hpf, indicating a transient requirement for blood flow in NA differentiation of SN precursors. We also found that blood flow affects NA differentiation indirectly, by promoting recruitment of Transgelin$^+$ VMCs. Three lines of evidence support this claim. First, blood-flow arrest inhibits DA coverage by Transgelin$^+$ VMCs during the exact same period when it affects NA differentiation of SNs. Second, inhibition of VMC differentiation via inhibition of PDGFR signaling inhibits NA differentiation in the presence of blood flow. Third, the presence of VMCs in *clo*^{s5} mutants is sufficient to drive normal SN development. These data support a model whereby the presence of VMC that coincides with the LDA-DA maturation is necessary for the proper NA differentiation of SN precursor cells, without affecting their neuronal differentiation.

VMC effects described here appear responsible only for part of the signaling from the DA, which takes place after the initial specification of SN precursors. In contrast, interfering with BMP signaling at the DA in the developing chick and mouse embryo is important for the attraction of neural crest cells and initial differentiation of SN progenitors (Reissmann et al., 1996; Schneider et al., 1999; Morikawa et al., 2009; Saito et al., 2012), suggesting the existence of a cascade of DA-derived signals. Interestingly however, SN differentiation can occur in zebrafish *clo*^{s5} mutants in absence of endothelial cells and blood flow, suggesting that the initial differentiation of SN progenitors is independent of factors derived from endothelial cells or the flowing blood and perhaps mediated by immature VMCs or other mesenchymal cells associated with the DA. Of note, we cannot formally exclude that besides VMCs, other, as-yet-unidentified cell types may participate to NA differentiation of SNs. Such demonstration will require selective ablation of VMCs or of genes directing VMC recruitment. While we show that PDGFR inhibition is sufficient to reduce DA coverage by Transgelin$^+$ VMCs, initial VMC assembly around pulmonary arteries in mice was shown to require PDGF and additional signaling pathways (Greif et al., 2012); therefore, more work is required to understand molecular mechanisms controlling VMC development.

The nature of the molecular signal derived from VMCs that induces NA differentiation of SN precursors is currently elusive. BMPs are likely candidates, since they are expressed in the DA of chicken (BMP-4/7; Reissmann et al., 1996; Saito et al., 2012), mouse (BMP-2/4; Shah et al., 1996), and zebrafish embryos (BMP-4; Stewart et al., 2010) and induce the expression of proneural genes and transcriptional regulators essential for SN development in vitro (Apostolova and Dechant, 2009). Analysis of BMP-2/4 and -7 expression in avian embryos revealed that cells expressing these markers were located in the DA on the innermost layer of cells as well as in the adjacent two or three cell layers before the onset of TH mRNA expression (Francis et al., 1994; Reissmann et al., 1996). However, BMPs are factors with high affinity binding to basement membranes (Dolez et al., 2011; Vukicevic et al., 1994), and the topographical organization of Zash-1a$^+$ progenitors aggregating adjacent to DA (Allende and Weinberg, 1994; Lucas et al., 2006; Shah et al., 1996) indicates

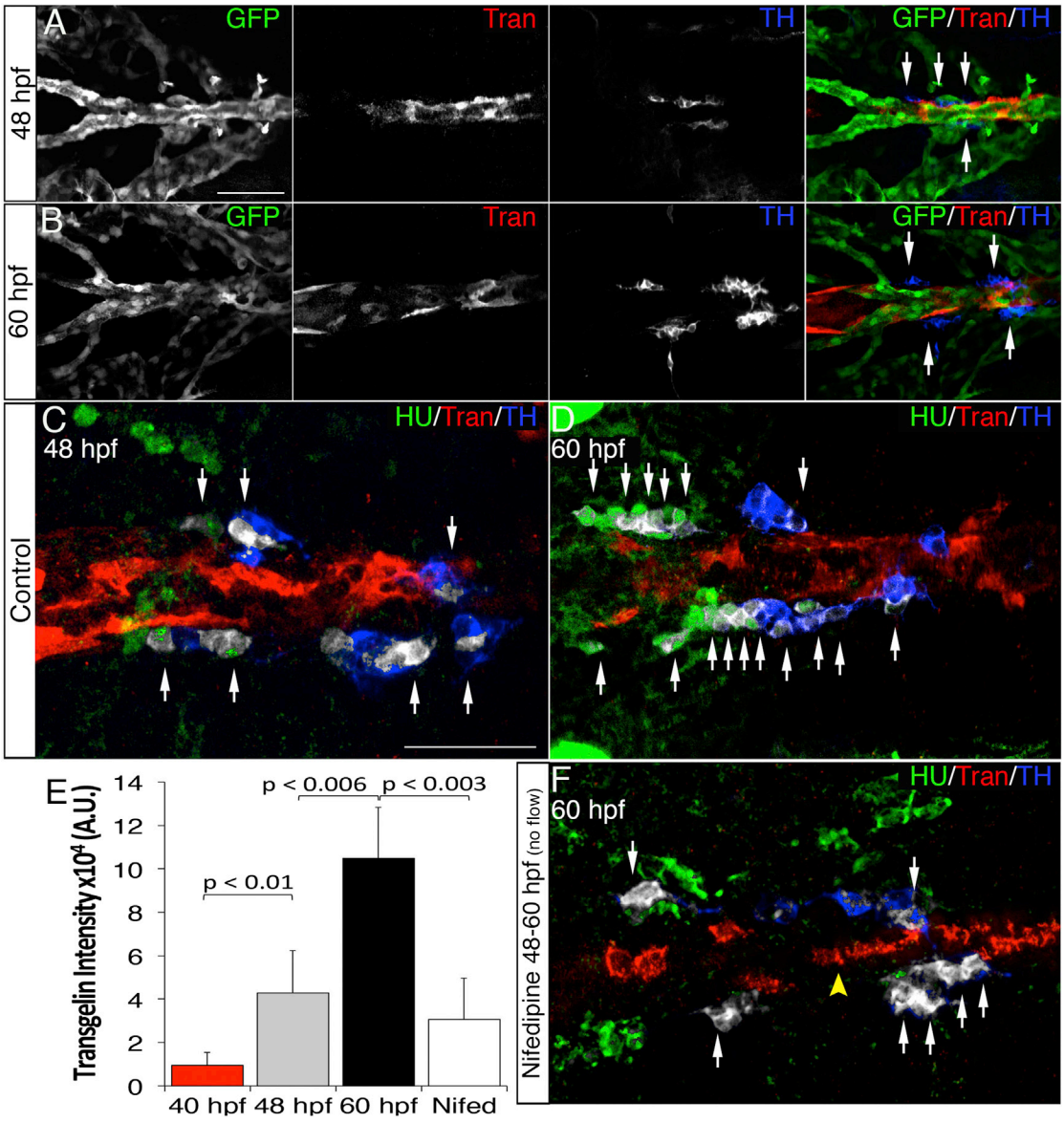

Figure 5. Blood Flow Triggers VMC Coverage and NA Differentiation

(A and B) Dorsal views (anterior is to the left) of whole-mount *Tg(kdrl:EGFP)*^{la116} zebrafish embryos immunostained with antibodies to detect GFP (endothelial cells, green), Transgelin (vascular mural cells, red), and TH (blue) at 48 (A) and 60 hpf (B). (A and B) Note appearance of Transgelin^{+} VMCs next to TH^{+} cells (arrows).

(C and D) HU^{+}/TH^{+} SNs (pseudocolored white) are next to VMCs (Transgelin^{+}, red) at 48 (C) and 60 hpf (D).

(E) Quantification of total Transgelin fluorescence intensity in control or 40 μM nifedipine-treated embryos. A.U., arbitrary units. Data were calculated from three independent experiments. Error bars indicate SD.

(F) Confocal images of *Tg(kdrl:EGFP)*^{la116} zebrafish embryos treated with 40 μM nifedipine for 12 hr starting at 48 hpf and immunostained for HU (green), Transgelin (red), and TH (blue). Note reduced VMC coverage and lower numbers of HU^{+}/TH^{+} SNs.

Scale bars, 75 μm (A–F). See also Figure S4.

that other candidate molecules might be involved. Moreover, it remains possible that DA endothelial and mural cells may express different types of BMPs.

A second environmental signal collaborates with BMP-2/4 to specify noradrenergic identity. In clonal culture of isolated murine NC stem cells, recombinant BMP-2/4 alone was unable to induce expression of TH, even though the expression of some panneural and specific autonomic genes was detected in 75% of the colonies (Shah et al., 1996). Avian NC cells in culture are responsive to BMPs 2/4/7 and increase the number of TH-expressing cells only in the presence of 10% total chick embryo extract (non-defined medium), which suggests that one or more molecules allow NC cells to develop to a point where they are responsive to the BMPs or in concert with the BMPs

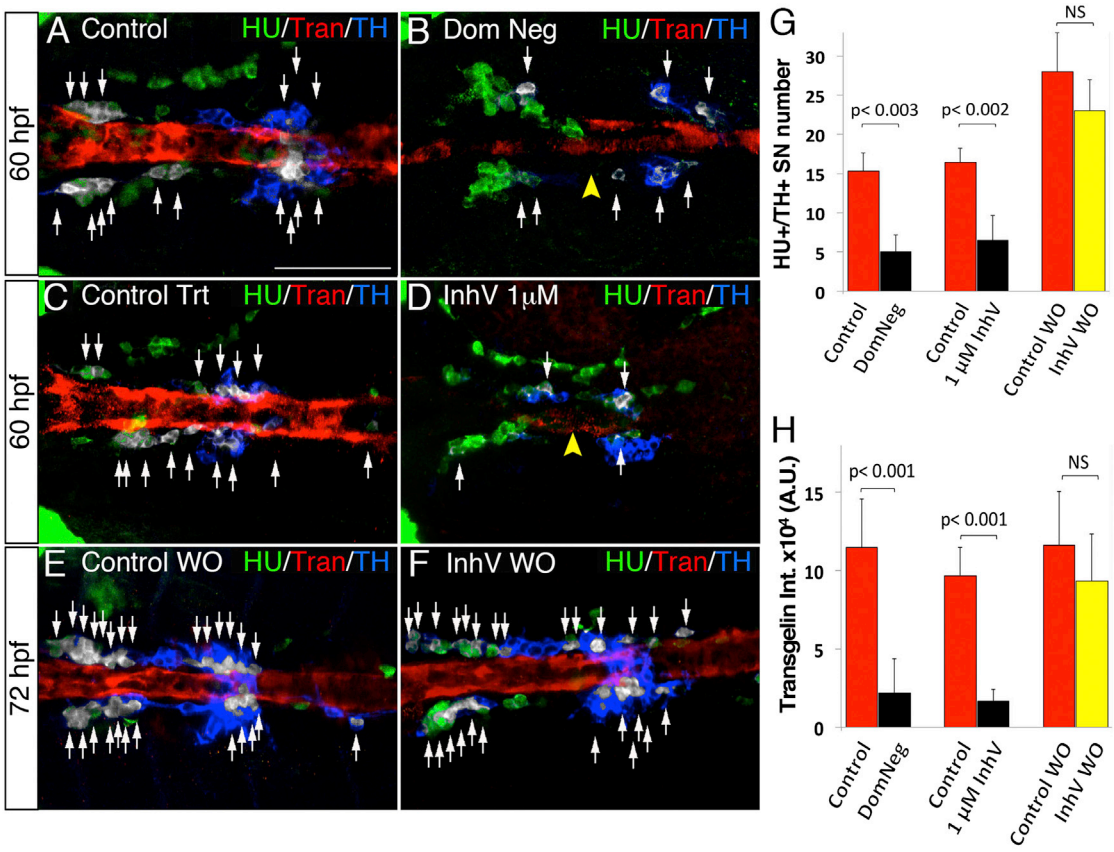

Figure 6. PDGF Inhibition Affects VMC Coverage and NA Differentiation

(A–F) Confocal analysis of *Tg(kdrl:EGFP)*^{la116} zebrafish embryos at the times indicated in the lateral panel and immunostained for HU (green), Transgelin (red), and TH (blue). Dorsal views (anterior is to the left). Arrows indicate white pseudocolored HU$^+$/TH$^+$ SNs. (A and B) Heat-shock embryos negative for dnPDGFRβ -YFP expression (A) and those heat-shock-induced embryos transiently expressing dnPDGFRβ-YFP (B) at 60 hpf. Arrowhead indicates the reduced VMC coverage in positive dnPDGFRβ-YFP embryos. (C and D) Control embryos treated with DMSO (C) or 1 μM of PDGFR inhibitor InhV (D) between 48 and 60 hpf. Arrowhead indicates the reduced VMC coverage in PDGFR inhibitor-treated embryos. Note presence of HU$^+$ cells but few HU$^+$/TH$^+$ SNs (D). (E and F) After 1 μM InhV exposure between 48 and 60 hpf, the drug was withdrawn and embryos were maintained in control conditions for an additional 12 hr (60–72 hpf). NA differentiation recovered following InhV withdrawal.

(G) Quantitative analysis of HU$^+$/TH$^+$ SNs.

(H) Quantitative analysis of Transgelin fluorescence intensity. Data were calculated from three independent experiments.

NS, not significant; error bars indicate SD. A.U., arbitrary units; hpf, hours post-fertilization. Scale bar, 75 μm (A–F). See also Figure S5.

to increase the number of TH$^+$ cells (Varley and Maxwell, 1996; Varley et al., 1995). Other studies have demonstrated that signaling pathways involving cyclic AMP (cAMP) and CREB are implicated in several aspects of SN development and demonstrate selective effects on the expression of TH and DβH (Lo et al., 1999; Rüdiger et al., 2009). Therefore, agents that stimulate cAMP/PKA levels may be directly involved in the development of noradrenergic sympathetic neurons (Pattyn et al., 2006).

We also show that DA endothelial cells do not affect NA differentiation of SNs, since this process occurs in the absence of endothelial cells in *clo*^{s5} mutants. VMCs in *clo*^{s5} mutants have been described previously in zebrafish around both the DA and visceral organs (Santoro et al., 2009), indicating that VMC specification can occur in the absence of blood flow and endothelial cells. Thus, blood vessels are not essential for VMC development, but they provide attractive signals that direct their recruitment to the vessel wall. VMC recruitment then triggers NA differentiation of adjacent SN precursors, revealing how neurovascular interactions between arteries and SNs are orchestrated during vertebrate development. Our experiments provide the basis for screening strategies designed to identify signals derived from VMCs that drive NA differentiation. Identification of such signals may lead to strategies to improve disease conditions associated with SN dysfunction.

EXPERIMENTAL PROCEDURES

Zebrafish Strains and Morpholinos

Zebrafish (*Danio rerio*) embryos and adults were maintained at 28.5°C on a 10-hr dark/14-hr light cycle and handled as described previously (Westerfield, 2000). Wild-type embryos were staged according to Kimmel et al. (1995). The Yale University Institutional Animal Care and Use Committee approved animal care and experimental use. Zebrafish lines were *Tg(kdrl:EGFP)*^{la116} (Choi et al., 2007), *Tg(kdrl:ras-mcherry)*^{s916}(Hogan et al., 2009), and *cloche(clo)*^{s5} (Stainier et al., 1995). The *Tg(dβh:EGFP)* line was kindly provided by

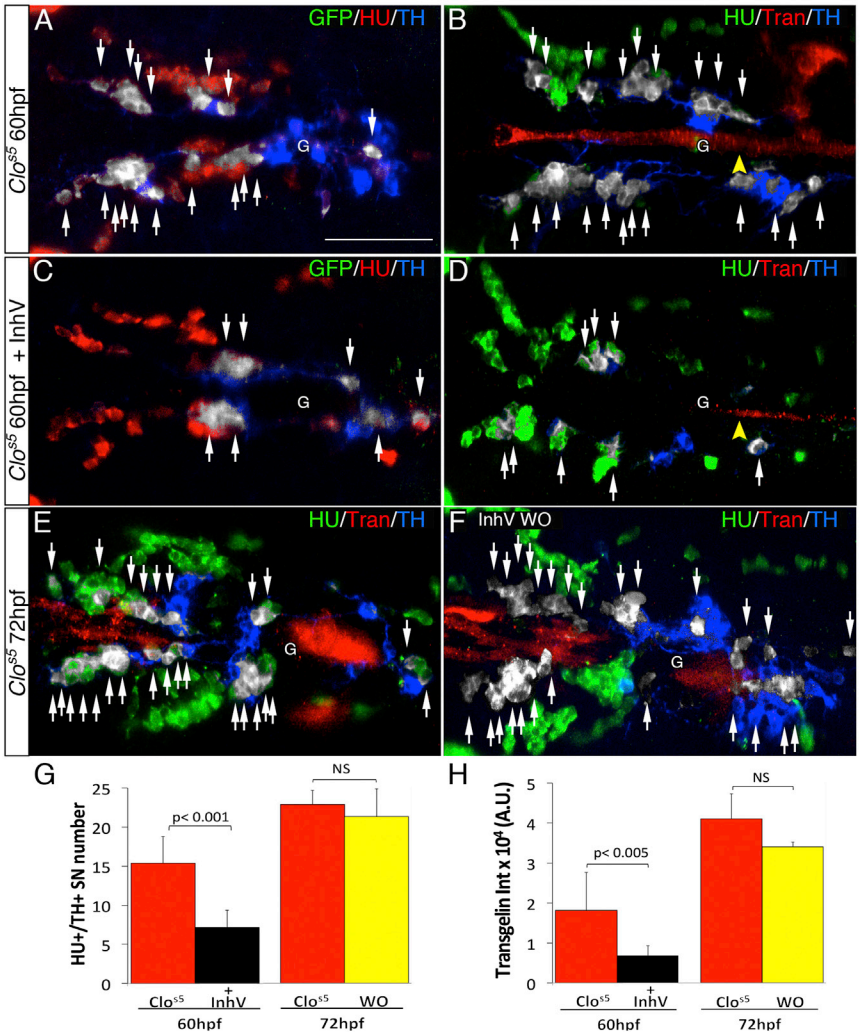

Figure 7. Ectopic VMCs in *clo*^{s5} Embryos Are Sufficient to Induce NA Differentiation

(A–F) Confocal analysis of *clo*^{s5} *Tg(kdrl:EGFP)* embryos. Dorsal views of the region between the LDA and the glomerulus (anterior is to the left). HU$^+$/TH$^+$ SNs are pseudocolored in white and indicated (arrows). (A and B) SNs develop in *clo*^{s5} mutant embryos in the absence of endothelial cells (A) and the presence of VMCs (B). Arrowhead indicates VMC coverage in *clo*^{s5} mutant embryos. (C and D) *clo*^{s5} embryos treated with 1 μM of PDGFR inhibitor InhV (D) or DMSO (C) between 48 and 60 hpf. Arrowhead indicates the reduced VMC coverage in *clo*^{s5} PDGFR inhibitor-treated embryos (D). Note presence of HU$^+$ cells but fewer HU$^+$/TH$^+$ SNs (white arrows) in *clo*^{s5} embryos treated with 1 μM PDGFR inhibitor. (E and F) *clo*^{s5} embryos treated with 1 μM of PDGFR inhibitor InhV between 48 and 60 hpf were maintained in control conditions for an additional 12 hr (60–72 hpf). SN morphogenesis and NA differentiation recovered following InhV withdrawal (F).

(G) Quantification of HU$^+$/TH$^+$ SNs in *clo*^{s5} mutant embryos.

(H) Quantitative analysis of Transgelin fluorescence intensity of the *clo*^{s5} mutant embryos. Data were calculated from three independent experiments.

NS, not significant; error bars indicate SD. A.U., arbitrary units; G, glomerulus; hpf, hours post-fertilization. Scale bar, 75 μm (A–F). See also Figure S6.

Dr. Thomas A. Look (Zhu et al., 2012). Double-transgenic *Tg(dβh:EGFP);(kdrl:ras-mcherry)*^{s916} embryos were selected at 48 hpf by mCherry and EGFP expression. Morpholinos (MOs) targeting *cardiac troponin T2* (*tnnt2*) (2 ng/embryo) (Sehnert et al., 2002) and a standard control MO (1–2 ng/embryo) (Bussmann et al., 2011) (Gene Tools) were injected into yolk of one- to two-cell-stage embryos. The inducible dominant-negative construct for pdgfrβ (dnpdgfrβ-YFP) (2 ng/embryo) (kindly provided by Dr. Lien) was injected at the one-cell stage as described previously (Wiens et al., 2010). 24-hpf embryos were heat shocked for 12 min in a 42°C water bath. Embryos with normal blood flow and overall morphology were selected and then sorted for YFP expression at 48 hpf.

Immunostaining

Whole-mount immunohistochemistry was performed as described previously (Inoue and Wittbrodt, 2011), with minor modifications. Briefly, embryos were fixed in 4% paraformaldehyde in PBS 0.1% Tween-20 (PBST), bleached in 3% H_2O_2, and stored in 100% methanol at −20°C. Fixed embryos were equilibrated in 150 mM Tris-HCl at pH 9.0 for 5 min, heated for 15 min at 70°C, and permeabilized in PBST and 100% acetone for 15 min at −20°C. Embryos were permeabilized with 15 μg/ml Proteinase K (PK) in PBST (48 hpf, 15 min; 60 hpf, 17 min; 72 hpf, 20 min). Embryos were blocked in 10% goat serum/PBST for 3 hr and incubated with primary antibodies in incubation buffer (1% Roche blocking reagent, 0.8% Triton X-100 in PBS) at 4°C overnight (ON). Embryos were rinsed and secondary antibody in incubation buffer was applied at 4°C ON. The larvae were washed in PBST and PBS and embedded in 1.5% low-melting agarose. Antibodies were Anti-HuC/D (elav3) (Molecular Probes; mouse monoclonal 16A11 antibody, 1:500) anti-TH (Abcam; sheep polyclonal antibody, 1:200), donkey-anti mouse-546 and donkey-anti sheep-647 secondary antibodies (Molecular Probes, 1:1,000), chicken-anti-GFP (Abcam, 1:300), donkey-anti-chicken-488 (Jackson ImmunoResearch Laboratories, 1:1,000), rabbit anti-Transgelin (Santoro et al., 2009; 1:100), and mouse anti-Zn12 (Zebrafish International Resource Center, 1:1,000).

Whole-Mount In Situ Hybridization and Drug Treatment

Whole-mount in situ hybridization was performed as described previously (Thisse and Thisse, 2008). Anti-sense RNA probes were synthesized by transcription of linearized cDNA clones with T7 or SP6 RNA polymerase using digoxigenin-labeling mix (Roche) and purified on spin columns (GE Healthcare Life Sciences). Riboprobes detected *zash-1a* (Lucas et al., 2006), *phox-2b*, pdgfr-β (Wang et al., 2014) *and th* (Stewart et al., 2006). To inhibit blood flow, embryos were treated with 40 μM Nifedipine (Sigma-Aldrich) (Li et al., 2008) or 20 mM BDM (Anderson et al., 2008) and incubated at 28.5°C for indicated time. For washout experiments, embryos were washed once with egg water and then transferred to medium without drug. PDGFR tyrosine kinase inhibitor V (InhV) was from Calbiochem (0.2–1.0 μM; Kim et al., 2010).

Image Acquisition, Processing, and Quantitative Analyses

Pigmentation of embryos was inhibited by MoTP (Sigma-Aldrich) (Yang and Johnson, 2006). Live embryos were treated with 100 μg/ml tricaine (Sigma-Aldrich), mounted in a drop of 1.0% low-melting agarose in egg water, and placed onto a glass-bottom dish. Confocal image stacks were acquired on a

Leica SP5 confocal microscope with ×25 or ×40 water-objective lenses (Leica Microsystems). Spatial distribution of co-localized pixels (pseudocolored white) was generated with plugin Colocalization_2 available for Fiji (NIH). Quantification of SNs was performed on confocal z stacks using Fiji Colocalization plugin. We assembled individual z stacks in Fiji and used single z planes to determine where the two channels overlapped. These values were summed to determine total SN number.

Statistical Analysis

At least three biological replicates were used for each data point and for derivation of error bars and SD. Data are expressed as mean ± SD. Statistical significance for paired samples and for multiple comparisons was determined by Student's t test and by Mann-Whitney non-parametric test, respectively. Data were considered statistically significant if the p value was less than 0.05.

SUPPLEMENTAL INFORMATION

Supplemental Information includes Supplemental Experimental Procedures and seven figures and can be found with this article online at http://dx.doi.org/10.1016/j.celrep.2015.05.028.

AUTHOR CONTRIBUTIONS

V.F., L.P., I.B., R.O., and E.R. performed experiments, M.M.S. contributed reagents, and V.F., S.N., and A.E. designed experiments and wrote the paper.

ACKNOWLEDGMENTS

We thank Jose Cardona and staff for animal husbandry, Thomas A. Look for the transgenic zebrafish strain, and Jean-Léon Thomas for helpful discussion. The study was supported by Fondation Leducq (Artemis Transatlantic Network of Excellence to A.E. and S.N.). V.F. was supported by the Brazilian National Council for Scientific and Technological Development (CNPq).

Received: March 15, 2014
Revised: April 14, 2015
Accepted: May 13, 2015
Published: June 11, 2015

REFERENCES

Allende, M.L., and Weinberg, E.S. (1994). The expression pattern of two zebrafish achaete-scute homolog (ash) genes is altered in the embryonic brain of the cyclops mutant. Dev. Biol. *166*, 509–530.

An, M., Luo, R., and Henion, P.D. (2002). Differentiation and maturation of zebrafish dorsal root and sympathetic ganglion neurons. J. Comp. Neurol. *446*, 267–275.

Anderson, M.J., Pham, V.N., Vogel, A.M., Weinstein, B.M., and Roman, B.L. (2008). Loss of unc45a precipitates arteriovenous shunting in the aortic arches. Dev. Biol. *318*, 258–267.

Apostolova, G., and Dechant, G. (2009). Development of neurotransmitter phenotypes in sympathetic neurons. Auton. Neurosci. *151*, 30–38.

Armulik, A., Abramsson, A., and Betsholtz, C. (2005). Endothelial/pericyte interactions. Circ. Res. *97*, 512–523.

Bronner-Fraser, M. (1986). Analysis of the early stages of trunk neural crest migration in avian embryos using monoclonal antibody HNK-1. Dev. Biol. *115*, 44–55.

Bussmann, J., Wolfe, S.A., and Siekmann, A.F. (2011). Arterial-venous network formation during brain vascularization involves hemodynamic regulation of chemokine signaling. Development *138*, 1717–1726.

Choi, J., Dong, L., Ahn, J., Dao, D., Hammerschmidt, M., and Chen, J.N. (2007). FoxH1 negatively modulates flk1 gene expression and vascular formation in zebrafish. Dev. Biol. *304*, 735–744.

Dolez, M., Nicolas, J.F., and Hirsinger, E. (2011). Laminins, via heparan sulfate proteoglycans, participate in zebrafish myotome morphogenesis by modulating the pattern of Bmp responsiveness. Development *138*, 97–106.

Eberhart, J.K., He, X., Swartz, M.E., Yan, Y.L., Song, H., Boling, T.C., Kunerth, A.K., Walker, M.B., Kimmel, C.B., and Postlethwait, J.H. (2008). MicroRNA Mirn140 modulates Pdgf signaling during palatogenesis. Nat. Genet. *40*, 290–298.

Flatmark, T. (2000). Catecholamine biosynthesis and physiological regulation in neuroendocrine cells. Acta Physiol. Scand. *168*, 1–17.

Francis, P.H., Richardson, M.K., Brickell, P.M., and Tickle, C. (1994). Bone morphogenetic proteins and a signalling pathway that controls patterning in the developing chick limb. Development *120*, 209–218.

Greif, D.M., Kumar, M., Lighthouse, J.K., Hum, J., An, A., Ding, L., Red-Horse, K., Espinoza, F.H., Olson, L., Offermanns, S., and Krasnow, M.A. (2012). Radial construction of an arterial wall. Dev. Cell *23*, 482–493.

Guo, S., Brush, J., Teraoka, H., Goddard, A., Wilson, S.W., Mullins, M.C., and Rosenthal, A. (1999). Development of noradrenergic neurons in the zebrafish hindbrain requires BMP, FGF8, and the homeodomain protein soulless/Phox2a. Neuron *24*, 555–566.

Hogan, B.M., Bos, F.L., Bussmann, J., Witte, M., Chi, N.C., Duckers, H.J., and Schulte-Merker, S. (2009). Ccbe1 is required for embryonic lymphangiogenesis and venous sprouting. Nat. Genet. *41*, 396–398.

Holzschuh, J., Barrallo-Gimeno, A., Ettl, A.K., Durr, K., Knapik, E.W., and Driever, W. (2003). Noradrenergic neurons in the zebrafish hindbrain are induced by retinoic acid and require tfap2a for expression of the neurotransmitter phenotype. Development *130*, 5741–5754.

Howard, M.J., Stanke, M., Schneider, C., Wu, X., and Rohrer, H. (2000). The transcription factor dHAND is a downstream effector of BMPs in sympathetic neuron specification. Development *127*, 4073–4081.

Inoue, D., and Wittbrodt, J. (2011). One for all—a highly efficient and versatile method for fluorescent immunostaining in fish embryos. PLoS ONE *6*, e19713.

Isogai, S., Lawson, N.D., Torrealday, S., Horiguchi, M., and Weinstein, B.M. (2003). Angiogenic network formation in the developing vertebrate trunk. Development *130*, 5281–5290.

Kasemeier-Kulesa, J.C., McLennan, R., Romine, M.H., Kulesa, P.M., and Lefcort, F. (2010). CXCR4 controls ventral migration of sympathetic precursor cells. J. Neurosci. *30*, 13078–13088.

Kim, J., Wu, Q., Zhang, Y., Wiens, K.M., Huang, Y., Rubin, N., Shimada, H., Handin, R.I., Chao, M.Y., Tuan, T.L., et al. (2010). PDGF signaling is required for epicardial function and blood vessel formation in regenerating zebrafish hearts. Proc. Natl. Acad. Sci. USA *107*, 17206–17210.

Kimmel, C.B., Ballard, W.W., Kimmel, S.R., Ullmann, B., and Schilling, T.F. (1995). Stages of embryonic development of the zebrafish. Dev. Dyn. *203*, 253–310.

Krispin, S., Nitzan, E., Kassem, Y., and Kalcheim, C. (2010). Evidence for a dynamic spatiotemporal fate map and early fate restrictions of premigratory avian neural crest. Development *137*, 585–595.

Kuntz, A. (1948). The autonomic nervous system. Prog. Neurol. Psychiatry *3*, 207–242.

Le Douarin, N.M., and Kalcheim, C. (1999). The Neural Crest, Second Edition (New York: Cambridge University Press).

Le Douarin, N.M., Smith, J., and Le Lièvre, C.S. (1981). From the neural crest to the ganglia of the peripheral nervous system. Annu. Rev. Physiol. *43*, 653–671.

Li, W.M., Webb, S.E., Chan, C.M., and Miller, A.L. (2008). Multiple roles of the furrow deepening Ca2+ transient during cytokinesis in zebrafish embryos. Dev. Biol. *316*, 228–248.

Lo, L., Morin, X., Brunet, J.F., and Anderson, D.J. (1999). Specification of neurotransmitter identity by Phox2 proteins in neural crest stem cells. Neuron *22*, 693–705.

Lucas, M.E., Müller, F., Rüdiger, R., Henion, P.D., and Rohrer, H. (2006). The bHLH transcription factor hand2 is essential for noradrenergic differentiation of sympathetic neurons. Development *133*, 4015–4024.

McKinney, M.C., Fukatsu, K., Morrison, J., McLennan, R., Bronner, M.E., and Kulesa, P.M. (2013). Evidence for dynamic rearrangements but lack of fate or position restrictions in premigratory avian trunk neural crest. Development *140*, 820–830.

McPherson, C.E., Varley, J.E., and Maxwell, G.D. (2000). Expression and regulation of type I BMP receptors during early avian sympathetic ganglion development. Dev. Biol. *221*, 220–232.

Morikawa, Y., Zehir, A., Maska, E., Deng, C., Schneider, M.D., Mishina, Y., and Cserjesi, P. (2009). BMP signaling regulates sympathetic nervous system development through Smad4-dependent and -independent pathways. Development *136*, 3575–3584.

Nicoli, S., Standley, C., Walker, P., Hurlstone, A., Fogarty, K.E., and Lawson, N.D. (2010). MicroRNA-mediated integration of haemodynamics and Vegf signalling during angiogenesis. Nature *464*, 1196–1200.

Nitzan, E., Krispin, S., Pfaltzgraff, E.R., Klar, A., Labosky, P.A., and Kalcheim, C. (2013). A dynamic code of dorsal neural tube genes regulates the segregation between neurogenic and melanogenic neural crest cells. Development *140*, 2269–2279.

Park, H.C., Kim, C.H., Bae, Y.K., Yeo, S.Y., Kim, S.H., Hong, S.K., Shin, J., Yoo, K.W., Hibi, M., Hirano, T., et al. (2000). Analysis of upstream elements in the HuC promoter leads to the establishment of transgenic zebrafish with fluorescent neurons. Dev. Biol. *227*, 279–293.

Pattyn, A., Guillemot, F., and Brunet, J.F. (2006). Delays in neuronal differentiation in Mash1/Ascl1 mutants. Dev. Biol. *295*, 67–75.

Raible, D.W., and Eisen, J.S. (1996). Regulative interactions in zebrafish neural crest. Development *122*, 501–507.

Reissmann, E., Ernsberger, U., Francis-West, P.H., Rueger, D., Brickell, P.M., and Rohrer, H. (1996). Involvement of bone morphogenetic protein-4 and bone morphogenetic protein-7 in the differentiation of the adrenergic phenotype in developing sympathetic neurons. Development *122*, 2079–2088.

Rohrer, H. (2011). Transcriptional control of differentiation and neurogenesis in autonomic ganglia. Eur. J. Neurosci. *34*, 1563–1573.

Rüdiger, R., Binder, E., Tsarovina, K., Schmidt, M., Reiff, T., Stubbusch, J., and Rohrer, H. (2009). In vivo role for CREB signaling in the noradrenergic differentiation of sympathetic neurons. Mol. Cell. Neurosci. *42*, 142–151.

Saito, D., Takase, Y., Murai, H., and Takahashi, Y. (2012). The dorsal aorta initiates a molecular cascade that instructs sympatho-adrenal specification. Science *336*, 1578–1581.

Santoro, M.M., Pesce, G., and Stainier, D.Y. (2009). Characterization of vascular mural cells during zebrafish development. Mech. Dev. *126*, 638–649.

Schneider, C., Wicht, H., Enderich, J., Wegner, M., and Rohrer, H. (1999). Bone morphogenetic proteins are required in vivo for the generation of sympathetic neurons. Neuron *24*, 861–870.

Sehnert, A.J., Huq, A., Weinstein, B.M., Walker, C., Fishman, M., and Stainier, D.Y. (2002). Cardiac troponin T is essential in sarcomere assembly and cardiac contractility. Nat. Genet. *31*, 106–110.

Seiler, C., Abrams, J., and Pack, M. (2010). Characterization of zebrafish intestinal smooth muscle development using a novel sm22α-b promoter. Dev. Dyn. *239*, 2806–2812.

Serluca, F.C., Drummond, I.A., and Fishman, M.C. (2002). Endothelial signaling in kidney morphogenesis: a role for hemodynamic forces. Curr. Biol. *12*, 492–497.

Shah, N.M., Groves, A.K., and Anderson, D.J. (1996). Alternative neural crest cell fates are instructively promoted by TGFbeta superfamily members. Cell *85*, 331–343.

Shtukmaster, S., Schier, M.C., Huber, K., Krispin, S., Kalcheim, C., and Unsicker, K. (2013). Sympathetic neurons and chromaffin cells share a common progenitor in the neural crest in vivo. Neural Dev. *8*, 12.

Siekmann, A.F., Standley, C., Fogarty, K.E., Wolfe, S.A., and Lawson, N.D. (2009). Chemokine signaling guides regional patterning of the first embryonic artery. Genes Dev. *23*, 2272–2277.

Stainier, D.Y., Weinstein, B.M., Detrich, H.W., 3rd, Zon, L.I., and Fishman, M.C. (1995). Cloche, an early acting zebrafish gene, is required by both the endothelial and hematopoietic lineages. Development *121*, 3141–3150.

Stern, C.D., Artinger, K.B., and Bronner-Fraser, M. (1991). Tissue interactions affecting the migration and differentiation of neural crest cells in the chick embryo. Development *113*, 207–216.

Stewart, R.A., Arduini, B.L., Berghmans, S., George, R.E., Kanki, J.P., Henion, P.D., and Look, A.T. (2006). Zebrafish foxd3 is selectively required for neural crest specification, migration and survival. Dev. Biol. *292*, 174–188.

Stewart, R.A., Lee, J.S., Lachnit, M., Look, A.T., Kanki, J.P., and Henion, P.D. (2010). Studying peripheral sympathetic nervous system development and neuroblastoma in zebrafish. Methods Cell Biol. *100*, 127–152.

Thisse, C., and Thisse, B. (2008). High-resolution in situ hybridization to whole-mount zebrafish embryos. Nat. Protoc. *3*, 59–69.

Tsarovina, K., Pattyn, A., Stubbusch, J., Müller, F., van der Wees, J., Schneider, C., Brunet, J.F., and Rohrer, H. (2004). Essential role of Gata transcription factors in sympathetic neuron development. Development *131*, 4775–4786.

Varley, J.E., and Maxwell, G.D. (1996). BMP-2 and BMP-4, but not BMP-6, increase the number of adrenergic cells which develop in quail trunk neural crest cultures. Exp. Neurol. *140*, 84–94.

Varley, J.E., Wehby, R.G., Rueger, D.C., and Maxwell, G.D. (1995). Number of adrenergic and islet-1 immunoreactive cells is increased in avian trunk neural crest cultures in the presence of human recombinant osteogenic protein-1. Dev. Dyn. *203*, 434–447.

Vukicevic, S., Latin, V., Chen, P., Batorsky, R., Reddi, A.H., and Sampath, T.K. (1994). Localization of osteogenic protein-1 (bone morphogenetic protein-7) during human embryonic development: high affinity binding to basement membranes. Biochem. Biophys. Res. Commun. *198*, 693–700.

Wang, Y., Pan, L., Moens, C.B., and Appel, B. (2014). Notch3 establishes brain vascular integrity by regulating pericyte number. Development *141*, 307–317.

Westerfield, M. (2000). The Zebrafish Book. A Guide for the Laboratory Use of Zebrafish (Danio rerio), Fourth Edition (University of Oregon Press).

Wiens, K.M., Lee, H.L., Shimada, H., Metcalf, A.E., Chao, M.Y., and Lien, C.L. (2010). Platelet-derived growth factor receptor beta is critical for zebrafish intersegmental vessel formation. PLoS ONE *5*, e11324.

Wildner, H., Gierl, M.S., Strehle, M., Pla, P., and Birchmeier, C. (2008). Insm1 (IA-1) is a crucial component of the transcriptional network that controls differentiation of the sympatho-adrenal lineage. Development *135*, 473–481.

Woldeyesus, M.T., Britsch, S., Riethmacher, D., Xu, L., Sonnenberg-Riethmacher, E., Abou-Rebyeh, F., Harvey, R., Caroni, P., and Birchmeier, C. (1999). Peripheral nervous system defects in erbB2 mutants following genetic rescue of heart development. Genes Dev. *13*, 2538–2548.

Yang, C.T., and Johnson, S.L. (2006). Small molecule-induced ablation and subsequent regeneration of larval zebrafish melanocytes. Development *133*, 3563–3573.

Young, H.M., Cane, K.N., and Anderson, C.R. (2011). Development of the autonomic nervous system: a comparative view. Auton. Neurosci. *165*, 10–27.

Zhu, S., Lee, J.S., Guo, F., Shin, J., Perez-Atayde, A.R., Kutok, J.L., Rodig, S.J., Neuberg, D.S., Helman, D., Feng, H., et al. (2012). Activated ALK collaborates with MYCN in neuroblastoma pathogenesis. Cancer Cell *21*, 362–373.